



CHEMISTRY & SUSTAINABILITY

CHEM **SUS** CHEM

ENERGY & MATERIALS

Accepted Article

Title: Excellent Performances of Dealuminated H-Beta Zeolites from Organotemplate-free Synthesis in Conversion of Biomass-derived 2,5-Dimethylfuran to Renewable p-Xylene

Authors: Rongrong Zhao, Zhenchao Zhao, Shikun Li, Andrei-Nicolae Parvulescu, Ulrich Müller, and Weiping Zhang

This manuscript has been accepted after peer review and appears as an Accepted Article online prior to editing, proofing, and formal publication of the final Version of Record (VoR). This work is currently citable by using the Digital Object Identifier (DOI) given below. The VoR will be published online in Early View as soon as possible and may be different to this Accepted Article as a result of editing. Readers should obtain the VoR from the journal website shown below when it is published to ensure accuracy of information. The authors are responsible for the content of this Accepted Article.

To be cited as: *ChemSusChem* 10.1002/cssc.201801504

Link to VoR: <http://dx.doi.org/10.1002/cssc.201801504>

WILEY-VCH

www.chemsuschem.org

A Journal of



Excellent Performances of Dealuminated H-Beta Zeolites from Organotemplate-free Synthesis in Conversion of Biomass-derived 2,5-Dimethylfuran to Renewable p-Xylene

Rongrong Zhao,^[a] Zhenchao Zhao,^[a] Shikun Li,^[a] Andrei-Nicolae Parvulescu,^[b] Ulrich Müller,^[b]* Weiping Zhang^{[a],*}

[a]State Key Laboratory of Fine Chemicals, School of Chemical Engineering, Dalian University of Technology, Dalian 116024, China

[b]BASF SE, Process Research and Chemical Engineering, 67056 Ludwigshafen, Germany

*Corresponding authors. E-mail: ulrich.mueller@basf.com (U.M.), wpzhang@dlut.edu.cn (W.Z.)

Abstract: Direct synthesis of renewable p-xylene (PX) via cycloaddition of biomass-derived 2,5-dimethylfuran (DMF) and ethylene was achieved on Al-rich H-Beta zeolites synthesized from organotemplate-free approach and their dealuminated counterparts with different Si/Al ratios. Among them, H-Beta zeolite with Si/Al ratio of 22 dealuminated from Al-rich parent was found to be an excellent catalyst for the production of p-xylene. The PX yield of 97 % and 2,5-DMF conversion of 99 % were obtained in the optimized conditions. These performances are even better than the commercial H-Beta zeolite from organotemplate synthesis with similar Si/Al ratio of 19. The excellent reaction activity of H-Beta zeolite with Si/Al ratio of 22 is closely related to its acidity and porous structure. A moderate Brønsted/Lewis acid ratio can improve the conversion of 2,5-DMF to as high as 99 %. Furthermore, dealuminated H-Beta zeolite possesses secondary pore system facilitating the diffusion of product, which increases the selectivity to PX. Besides, this catalyst demonstrates better regeneration. After five successive regeneration cycles, the yield of PX is still as high as 85 % without obvious dealumination. This work provides a deeper understanding of the more general Diels–Alder cycloaddition of furan-based feedstocks and olefins, and significantly improves the potential for the production of sustainable chemicals from lignocellulosic biomass.

Keywords: Renewable p-xylene; Biomass-derived 2,5-Dimethylfuran; Dealuminated H-Beta zeolites; Sustainable chemicals

Introduction

The sustainable production of widely used bulk chemicals from biomass has received great attention due to the high cost, market volatility and impending depletion of petroleum-based feedstocks.^[1-4] p-Xylene (PX) is one of the most important specific chemicals of interest since it is extensively used to produce terephthalic acid (TA), polyethylene terephthalate (PET), and subsequent synthesis of polyester, synthetic fibers and plastic bottles, etc. A promising pathway for the production of renewable p-xylene, using Diels-Alder reaction between ethylene and 2,5-dimethylfuran (2,5-DMF), have been proposed in recent years.^[5-9] Both 2,5-DMF^[10, 11] and ethylene^[12] can be derived from biomass, which is potential to reduce the dependence on petroleum.

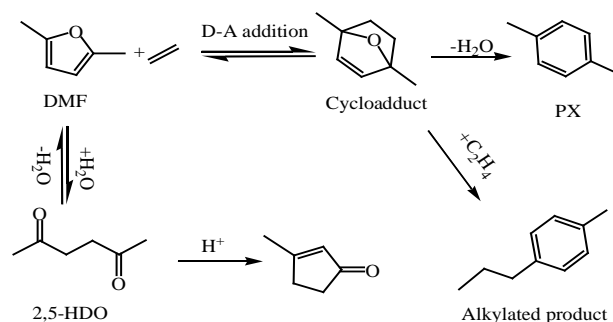
The reaction activities between 2,5-DMF and ethylene rely not only on the catalyst acid strength and amount, but also on the acid type. Williams et al.^[13] reported a selectivity of ~75 % to PX over H-Y zeolite. Chang et al.^[8] demonstrated that using commercial H-Beta zeolite, PX selectivity can reach 90 %. Nikbin et al.^[6, 7] suggested that Brönsted acid sites in the solid catalyst are active for PX production while the Lewis acid sites are less reactive for the dehydration of cycloadduct both from experimental studies and DFT calculations. And with amorphous $\text{WO}_x\text{-ZrO}_2$ and niobic acid, Wang et al.^[14] also showed that the Brönsted acidity is essential for the dehydration of the adduct. However, other reports claimed that only Lewis acid can also catalyze this reaction.^[15, 16] For instance, Chang et al.^[15] demonstrated that Zr-, Sn-, or Ti-Beta zeolite with only Lewis acidity can produce PX from 2,5-DMF and ethylene similarly to that of the Brönsted acid catalysts. Therefore, the acid type has great influence on this reaction. As a major solid-acid catalyst, zeolites have both Brönsted and Lewis acid sites and their acidity can be finely tuned through post-treatings. Among them dealumination by acid leaching and/or steaming is demonstrated to alter the acid amount and strength.^[17, 18] What's more, dealumination is generally applied to increase the zeolites thermal stability and to create secondary pore system, which enables shorter diffusion paths and improve the catalyst performances.^[19-21] Although Beta zeolites exhibit excellent performances in many catalytic reactions, their wide applications in chemical industry are sometimes challenging due to the use of organic templates in the synthesis. This would not only increase the cost of zeolite production but also result in consumption of energy and pollution for the environment caused by the removal of organic templates at high-temperature calcination. Beta zeolites synthesized from organotemplate-free approach not only overcome these drawbacks but also enrich the framework aluminum content with Si/Al ratio down to

around 4.6.^[22-24] These provide great opportunities to regulate the Brønsted/Lewis acidity and porosity of Beta zeolites through dealumination of the Al-rich counterpart. Indeed, organotemplate-free Beta zeolites with a large number of Brønsted acid sites are effective in cracking of cumene^[25] and NH₃-SCR of NO_x when introducing Cu or Fe.^[26, 27] Meanwhile the dealuminated ones are more active and delay the deactivation in the alkylation and acylation,^[28] methanol to olefins,^[29, 30] glucose to 5-hydroxymethylfurfural,^[31] n-hexane cracking.^[32] However, up to date there is little study on the catalysis of organotemplate-free Al-rich Beta zeolites in the conversion of biomass platform molecules to widely used bulk chemicals.

Herein, this work reports the commonly used platform molecule 2,5-DMF reacts with ethylene through Diels–Alder cycloaddition, and then dehydrated to produce PX over organotemplate-free Beta and derived dealuminated zeolites, which exhibit excellent catalytic performances. The influences of Brønsted/Lewis acid ratio, porosity and regeneration of used catalysts are investigated in details. The structure-reactivity correlation is elucidated through the comparison with the conventional Beta zeolites from organotemplate synthesis. Moreover, other derivatives methylfuran/furan with ethylene to produce toluene and benzene are also tested on the optimized zeolite.

Results and discussion

Al-rich HBeta zeolite from organotemplate-free synthesis can efficiently catalyze 2,5-DMF and ethylene to produce the main product paraxylene. Additionally other compounds were also detected and further identified by GC/MS (see Figure S1-S2, Supporting Information). Based on these information, the detailed reaction network of 2,5-DMF and ethylene in our catalytic system is exhibited in Scheme 1. Similar to the network proposed by other groups,^[8, 9] besides the Diels–Alder cycloaddition of 2,5-DMF with ethylene and subsequent dehydration to the targeted product PX, the hydrolysis of 2,5-DMF to 2,5-hexanedione (2,5-HDO) which easily dehydrated to 3-methyl-2-cyclopentenone, side-chain alkylation of PX to 1-methyl-4-propylbenzene, and the incompletely dehydrated cycloadduct are the main side products. Among them 1-methyl-4-propylbenzene is detected, which is different from the result from Williams et al. where they found 1-ethyl-2,5-dimethylbenzene.^[13] In order to improve the catalyst activity and PX selectivity, the reaction conditions were optimized using Al-rich H-Beta zeolite (Si/Al=7).



Scheme 1 Reaction network leading to p-xylene and byproducts from 2,5-dimethylfuran (DMF) and ethylene

Effect of reaction temperature

The effect of temperature on the reaction activity was investigated in the range of 200-320 °C. It is known from Figure 1 that as the reaction temperature increases from 200 to 300 °C, DMF conversion increases from 61 to 89 %, and the yield to PX increases from 54 to 77 %. Besides, the main byproduct changes from the incomplete dehydration cycloadduct to alkylated compound. And when the temperature is as high as 300 °C, the selectivity to cycloadduct is lower than 1 %. However, a further increase of reaction temperature from 300 to 320 °C, the PX yield decreases to 72 %. This is due to more alkylated product generated at higher temperatures. Considering the PX yield, the optimized reaction temperature is 300 °C.

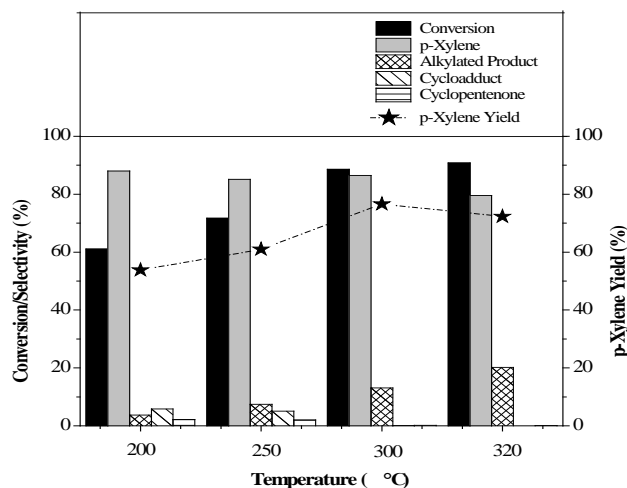


Figure 1 Effect of temperature on DMF and ethylene to PX in heptane over H-Beta zeolite (catalyst weight=0.3 g, $C_{2,5\text{-DMF}}=1.56$ M, $P_{\text{initial}}=3.0$ MPa, $t=20$ h).

Effect of 2,5-DMF concentration

The reactant concentration is another important parameter for the reaction activity. The concentrations of

DMF in solvent n-heptane varied from 0.78 to 3.12 M. As shown in Figure 2, the side reactions are predominantly caused by the alkylation of PX. DMF conversion decreases from 98 to 60 % as its concentration increases to 3.12 M. The selectivity to p-xylene changes slightly under different DMF concentrations while p-xylene yield decreases from 78 to 50 %. Under the same amount of catalyst, a higher concentration of reactant means lower Brønsted acid sites per cycloadduct molecule can access, leading to a reduction in the rate of dehydration reaction. Because the Diels-Alder reaction is reversible, the decrease in the dehydration rate also decreases the rate of first-step reaction, and further results in a reduction in DMF conversion. Besides, a lower concentration of DMF in the reactant system leads to higher selectivity to the alkylated product (Figure 2). Therefore, an appropriate DMF concentration in heptane could be 1.56 M in consideration of its conversion and the purification of the product.

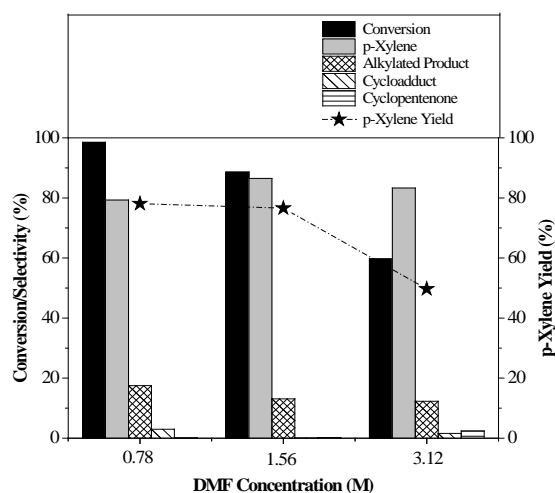


Figure 2 Effect of DMF concentration in heptane on DMF and ethylene to PX over H-Beta zeolite (catalyst weight=0.3 g, T =300 °C, P_{initial}= 3.0 MPa , t = 20 h).

Effect of ethylene pressure

To investigate the impact of ethylene pressure on reaction activity, its initial pressure was varied from 1.0 to 4.0 MPa. In Figure 3, it is found the reaction rate is proportional to the initial ethylene pressure. When the pressure increases to 4.0 MPa, DMF conversion increases to 96 %. The main byproduct is cycloadduct when the ethylene pressure is 1.0 MPa. While the alkylated product becomes dominant when its pressure is higher than 1.0 MPa. A higher initial ethylene pressure doesn't have a significant influence on the product selectivity but is beneficial to reaction rate. Nevertheless, the initial ethylene pressure is set to 4 MPa in view of the safety of the equipment as much higher system pressure reaches after heating to

300 °C.

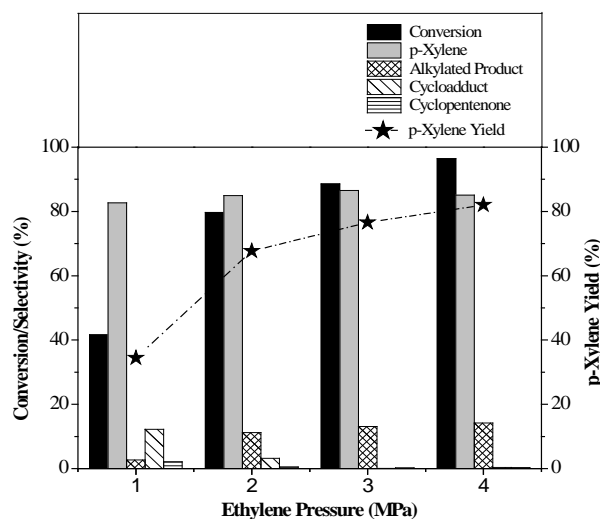


Figure 3 Effect of initial ethylene pressure on DMF and ethylene to PX over H-Beta zeolite (catalyst weight=0.3 g, $C_{2,5}$ -DMF = 1.56 M, T =300 °C, t = 20 h).

Effect of reaction time

Reaction time may have an impact on the catalytic performances of H-Beta zeolite. As shown in Figure 4, reaction time varies from 10 to 20 h, DMF conversion improves from 83 % to 96 % leading to p-xylene yield increase by 15 %. Further prolonging reaction time to 30 h, no improvement for p-xylene yield is observed. Besides, changing reaction time has no big influence on the selectivity to p-xylene. For all the reactions after different hours, the selectivity to alkylated product is about 15 %. Thus, the optimized reaction time could be 20 h. As the mechanism reported by Do et al.^[5] the formation of alkylated product competes with that of p-xylene, which is caused by the secondary reaction after p-xylene has been formed. It seems that reaction time has effect on the DMF conversion while makes nearly no difference on the byproducts. Thus, to decrease the selectivity to the byproducts, especially alkylated product, HBeta zeolite with appropriate properties should be selected.

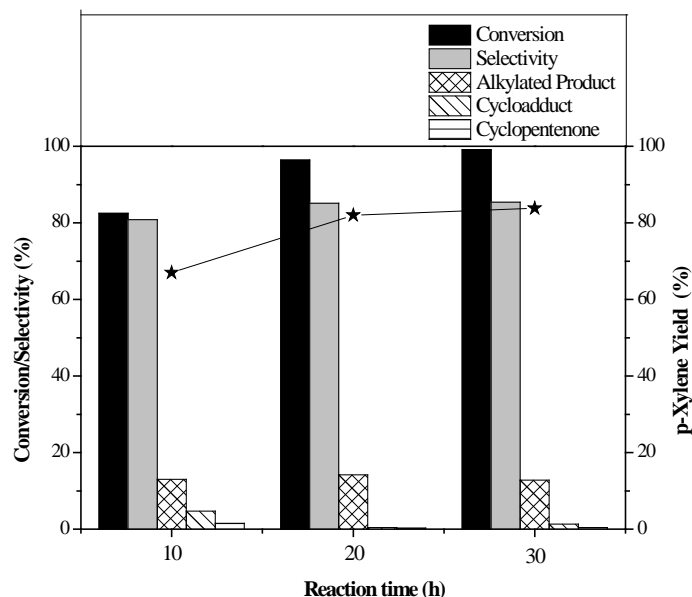


Figure 4 Effect of reaction time on DMF and ethylene to PX over H-Beta zeolite (catalyst weight=0.3 g, $C_{2,5-DMF} = 1.56$ M, $T = 300$ °C, $P_{initial} = 4.0$ MPa).

Effect of Si/Al ratios

The reaction network and the mechanism of DMF and ethylene show that the catalyst acidity is vital for the production of p-xylene. For H-Beta zeolite, the properties of acid sites are directly determined by the Al distributions and contents. Therefore, it's necessary to investigate the influence of Si/Al ratios on the reaction performances. As shown in Figure 5, both H-Beta zeolite with Si/Al ratio of 7 and 36 have higher selectivity to the alkylated product, thus decreasing the selectivity to PX. While H-Beta zeolites with Si/Al ratio of 19 and 22 have much less alkylated product and much higher PX yields. It is worth noting that the dealuminated H-Beta with Si/Al of 22 from the Al-rich parent has better DMF conversion and PX yield than the commercial one with Si/Al of 19 from organotemplate synthesis. Under the optimized conditions PX yield of 97 % and DMF conversion of 99 % are obtained on dealuminated H-Beta with Si/Al of 22, higher than H-Beta zeolite and Zr-Beta zeolite reported by Chang et al. ^[8, 15] after reaction for 20 h. Although both zeolites have similar Si/Al ratio, their catalytic performances are different in the conversion of DMF and ethylene to PX. This may be related to the acidity property and local structure of H-Beta zeolites from different preparation approaches as revealed by the following characterizations.

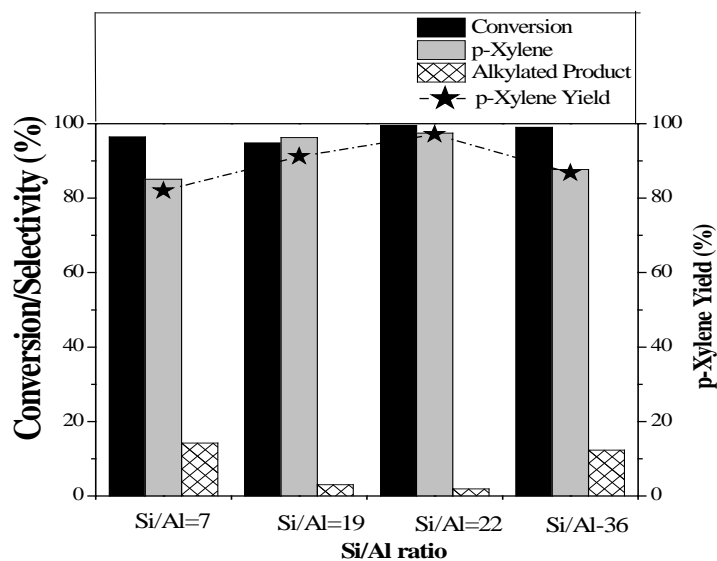


Figure 5 Effect of Si/Al ratios on DMF and ethylene to PX over H-Beta zeolites (catalyst weight=0.3 g, $C_{2,5-DMF}$ =1.56 M, T =300 °C, $P_{initial}$ =4.0 MPa, t =20 h).

Acidity Characterization

The reaction activity between DMF and ethylene relies not only on the quantity and strength of acid sites, but also on the acid type (Brönsted or Lewis acid site). While the Brönsted and Lewis acid sites in zeolites are correlated to the specific types of aluminum species,^[33] thus, the H-Beta zeolites with different Si/Al ratios would have different acid features, such as acid strength, amount and Brönsted/Lewis site (B/L) ratio. Figure 6a shows the NH_3 temperature-programmed desorption (TPD) profiles of H-Beta zeolites with different Si/Al ratios. It is clear that the overall acid amount of H-Beta-7 is much higher than the others since it is Al-rich one, which is in line with ^{27}Al MAS NMR spectra shown in Figure S3 that the content of framework Al for H-Beta-7 is much higher than the others and less extra-framework Al appears. After deconvoluting the profiles (Figure 6b), all samples show three desorption peaks centered at *ca.* 200 °C (low temperature), 250 °C (middle temperature) and 340 °C (high temperature), respectively. The latter two peaks could be roughly attributed to NH_3 desorption on strong and weak Brönsted acid sites, while the low-temperature peak could be probably assigned to NH_3 desorption on Lewis acid sites.^[34-36] Thus the approximate B/L ratio can be calculated through the integration of desorption signals, which is listed in Table 1. It is clear that the B/L ratios for H-Beta-7 and H-Beta-19 are higher than those for H-Beta-22 and H-Beta-36. Moreover, the desorption temperature varies with the Si/Al ratio of H-Beta zeolite, especially

the ammonia desorption on weak Brönsted acid sites. For H-Beta-7, the desorption temperature is 235 °C, with increasing Si/Al ratio it increases to 260 °C, while for the other two peaks, it hardly changes. Thus, for H-Beta zeolite the higher the Si/Al ratio is, the stronger the acid strength is.

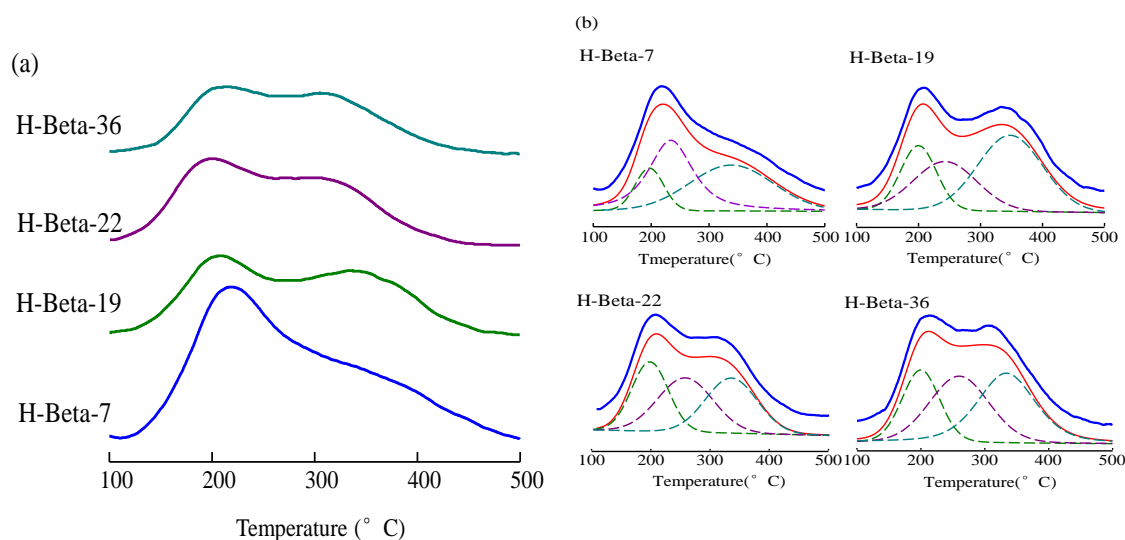


Figure 6 NH₃-TPD profiles (a) and corresponding deconvoluted spectra (b) of H-Beta zeolites with different Si/Al ratios after NH₃ adsorption.

To get more insights into the acid amount and strength of H-Beta zeolites with different Si/Al ratios, ³¹P MAS NMR experiments are conducted, which is an effective tool to investigate the acidic properties using trimethylphosphine oxide (TMPO) as a probe molecule.^[37, 38] Not only the acid sites types (Brönsted acid or Lewis acid) can be distinguished, ³¹P-TMPO MAS NMR approach is also more useful for discriminating the Brönsted acid strength of zeolite catalysts and capable of covering the whole range from weak, medium, strong to superacidity.^[39] As shown in Figure 7, the ³¹P MAS NMR line shape between H-Beta-22 and H-Beta-19 is quite different although these two samples have similar Si/Al ratio, which means they could have different acidity distribution. After deconvolution there are seven peaks appeared from the low to high field. Besides the physisorbed TMPO at around 43 ppm, the ³¹P NMR chemical shifts from 50 to 84 ppm are ascribed to chemical adsorbed TMPO on Brönsted or Lewis acid sites.^[40-42] According to our previous study,^[42] the peaks at ca. 83, 69 and 55-62 ppm are assigned to TMPO adsorbed on the strongest, medium-strength and weakest Brönsted acid sites, respectively. While those at 65 and 50 ppm are ascribed to TMPO adsorbed on the Lewis acid sites. It is clear from Figure 6 that H-Beta-22 from dealumination of Al-rich H-Beta-7 has more medium-strength Brönsted acid sites than the commercial H-Beta-19. After

quantification the total amount of Brönsted and Lewis acid sites, and B/L ratios are listed in Table 1. It is found that the higher Si/Al ratio is, the less amount of Brönsted acid sites is. The B/L ratio decreases then increases with increasing the Si/Al ratio, which is in line with the result from NH_3 -TPD. It is worth noting that H-Beta-22 has smaller B/L ratio than H-Beta-19, indicating H-Beta-22 has more Lewis acid sites although they have similar Si/Al ratio.

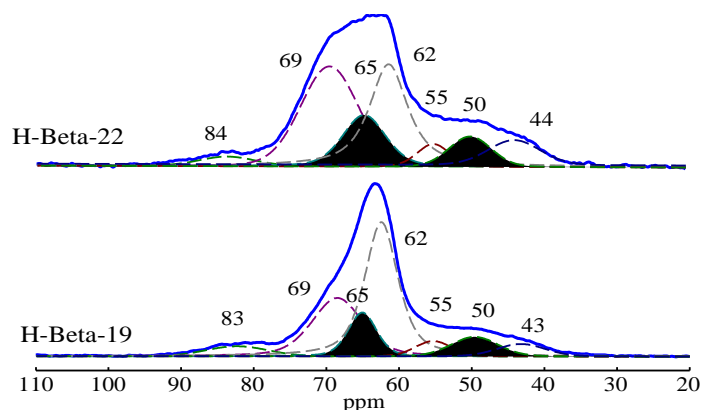


Figure 7 ^{31}P MAS NMR spectra of H-Beta zeolites with Si/Al ratio of 19 and 22 after TMPO adsorption. The shaded peaks represent resonances associated with Lewis acid sites.

Table 1 Si/Al ratios, acid site amount, surface areas and pore volumes of different H-Beta zeolites

Catalyst	Si/Al ratio	B/L from NH_3 -TPD	Brönsted acid ($\mu\text{mol/g}$)	Lewis acid ($\mu\text{mol/g}$)	B/L from ^{31}P MAS NMR	BET surface area (m^2/g)	Total pore volume (cm^3/g)
H-Beta-7	7	7.0	956	110	8.7	449	0.31
H-Beta-19	19	4.0	527	136	4.0	520	0.36
H-Beta-22	22	2.3	448	185	2.4	500	0.36
H-Beta-36	36	3.0	289	106	2.7	548	0.38

Porosity characterization

^{29}Si MAS NMR spectra (Figure S4) show that for H-Beta-22 zeolite, the intensity of silanols (Si-OH) is much higher than H-Beta-19 zeolite, indicating more defective sites in H-Beta-22 since it came from

dealumination of Al-rich H-Beta-7 while H-Beta-9 was obtained by direct synthesis. This implies their porosity may be different. From nitrogen physisorption characterization, all samples showed characteristic of type I adsorption-desorption isotherms without the presence of hysteresis loops (See Figure S5), and there are no obvious differences of the BET surface areas and pore volumes among the samples (Table S1). Thus, N₂ physisorption is not sensitive to detect the porosity difference for the samples especially H-Beta-22 and H-Beta-19.

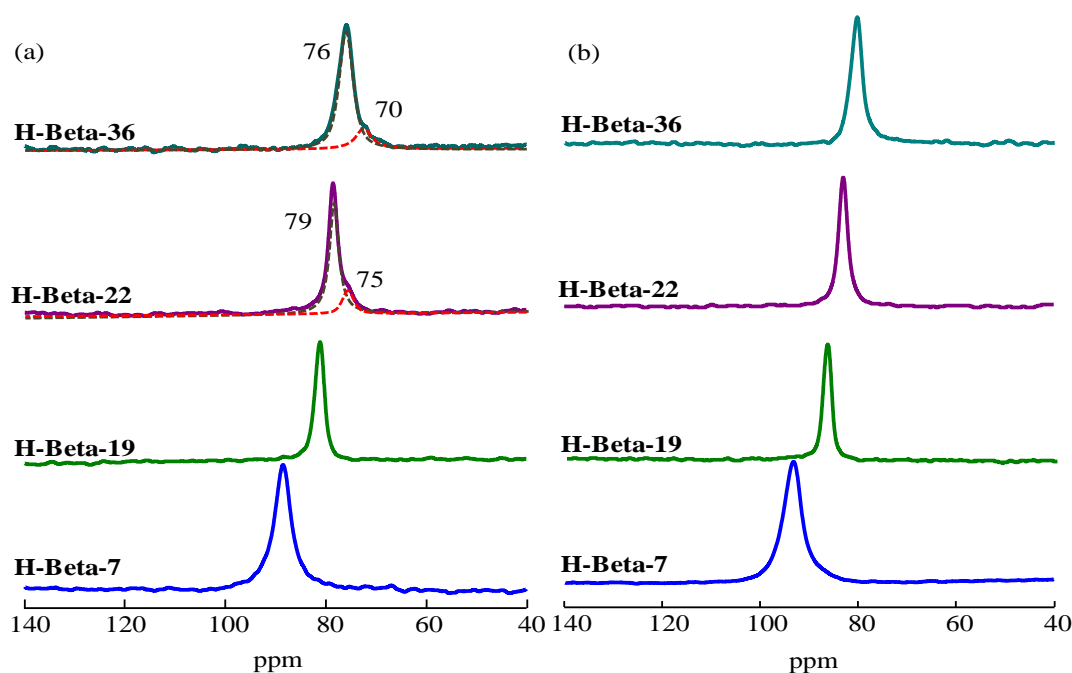


Figure 8 ^{129}Xe MAS NMR spectra of H-Beta zeolite with different Si/Al ratios under equilibrium pressure of 70 Torr (a) and 140 Torr (b) at a magic-angle-spinning rate of 5 kHz.

^{129}Xe NMR spectroscopy is a unique and sensitive technique for investigating the porous structures of solid materials especially for microporous zeolites.^[43] To get more details on the porosity of H-Beta zeolites with different Si/Al ratios, ^{129}Xe NMR without magic-angle spinning (MAS) was investigated under low pressures as shown in Figure S6. To suppress the effect of anisotropic chemical shift and achieve higher resolution, ^{129}Xe MAS NMR at 5 kHz were further conducted. From Figure 8, it is found that under the same xenon adsorption pressure, the chemical shifts increase linearly with the framework Al content in H-Beta zeolite. This may be due to the stronger Xe-surface interaction as the Si/Al ratio decreases, which agrees well with what we found in dealuminated H-ZSM-5.^[44] At low xenon adsorption pressure, only one peak is observed for H-Beta-7 and H-Beta-19 zeolites owing to xenon adsorbed in the 12-MR pore of Beta.

While for H-Beta-22 and H-Beta-36 zeolites from dealumination of H-Beta-7, besides the main signal an extra peak appears at high field with chemical-shift difference of ca. 5 ppm. Based on the fact that only one xenon signal in the primary 12-MR pore appears in H-Beta-7 and H-Beta-19 zeolites from direct synthesis, the second peak at high field should be caused by the dealumination, which slightly expands the 12-MR leading to weakening the xenon-xenon interaction. So, H-Beta-22 and H-Beta-36 zeolites have both primary and secondary pores. By simulating and integrating the Xe NMR signals, the content of secondary pores can reach about 10 % for these zeolites. The secondary porosity created by dealumination has also been observed in Y and Mordenite zeolites.^[45, 46] After increasing the xenon adsorption pressure, the two ¹²⁹Xe NMR signals merge into a single one in H-Beta-22 and H-Beta-36 zeolites. This could be caused by the faster xenon exchange between the primary and secondary pores.

Combining the acidity and porosity characterizations with the catalytic performances, it is known that for H-Beta zeolite with Si/Al ratio of 7, 22 and 36, H-Beta-22 has higher selectivity of PX than the others, while the quantity of Brönsted acid sites for H-Beta-7 is much higher than others. The excess amount of Brönsted acid sites would increase the selectivity to byproducts leading to the decrease in PX selectivity as mentioned above. While for H-Beta-36, the stronger Brönsted acid strength is negative for the selectivity to PX, agreeing with the computational study^[47] that for dehydration process, reaction rate is determined by deprotonation. H-Beta-22 zeolite owns moderate Brönsted acid strength. This may result in better catalytic performances for H-Beta-22 than H-Beta-7 and H-Beta-36. Additionally, H-Beta-22 has even higher reaction performances than commercial H-Beta-19 although they have similar Si/Al ratio. From the acidity and porosity characterizations these two H-Beta zeolites have similar acid strength, but H-Beta-22 has more Lewis acid sites and also has the secondary porous structure. Nikbin et al.^[6, 7] reported that Lewis acid sites are not effective at catalyzing the dehydration of the cycloadduct but more active to catalyze the Diels–Alder reaction compared to Brönsted acid sites, therefore, the bifunctional H-Beta zeolite both has Lewis and Brönsted acid sites can accelerate the cycloaddition and the dehydrative aromatization, respectively. In order to understand the role of Lewis acid sites in our case, the extraframework Al in H-Beta-22 was removed by washing using diluted HCl solution. As seen in ²⁷Al MAS NMR spectrum (Figure S7), the signal of non-framework Al decreases dramatically while no change occurs on framework Al after acid treatment. Nevertheless, the extraframework Al can not be fully removed since there is a weak signal at 0 ppm after repeated washing by HCl solution, which is the usual case in Beta zeolite and reported by many other groups.^[48, 49] After removing most extraframework Al in H-Beta-22 zeolite, it shows reduced

PX selectivity to 89 % while a little decline of 2,5-DMF conversion, leading to the obvious decrease of PX yield from 97 % to 86 % (Figure S8). Thus, the presence of Lewis acid sites in H-Beta-22 zeolite is beneficial to the improvement of PX selectivity by decreasing the selectivity to byproduct especially alkylated product. Besides, the generation of secondary pore system in the H-Beta-22 zeolite would facilitate the diffusion of reactants and products, increasing 2,5-DMF conversion and PX yield. The moderate acid property and porous structure make H-Beta-22 zeolite a superior catalyst for the conversion of DMF and ethylene to PX.

Successive regeneration of spent H-Beta zeolite

After a long time reaction (~20 h) in the autoclave there are coke deposits in H-Beta-22 catalyst. The regeneration of spent catalyst is very important for practical applications. Coke deposits can be eliminated by oxygen treatment at high temperature.^[50] Figure 9 shows that the catalytic activity can be properly restored after regeneration. The DMF conversion and PX selectivity decrease gradually with regeneration cycles. After 6 successive regeneration cycles, DMF conversion reduces slightly from 99 to 96 %, while PX selectivity decreases considerably from 97 to 85 %. The main byproducts are the alkylated product and furan derivatives caused by the incomplete dehydration of cycloadduct. ²⁷Al MAS NMR spectra in Figure S9 show that carbon deposits lead to broadening the framework Al signal. After regeneration the line width of framework Al at 55 ppm can not be fully restored to the fresh catalyst. After regeneration for six times, the intensity of framework Al reduces greatly and the extraframework Al at around -5 ppm increases obviously, which indicates that a part of framework Al has been released from the zeolite lattice. Correlating to the catalytic performance in Figure 9, it is clear that after successive regeneration for 6 times the dealumination of H-Beta-22 occurs, which decreases the amount of Brønsted acid sites causing the decline of selectivity to PX, and the selectivity to the incomplete hydrolysis byproduct increases.

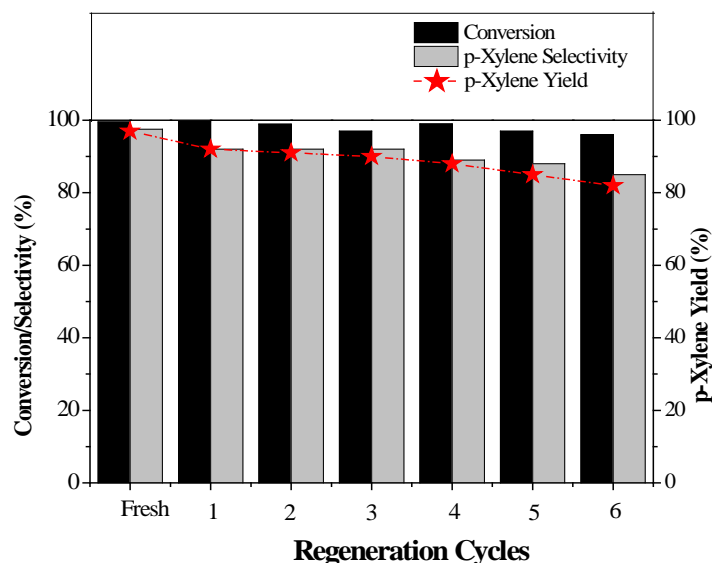


Figure 9 Catalytic performances of spent H-Beta-22 zeolite after successive regeneration cycles

To evaluate the content of carbonaceous deposits, TG analysis was carried out for H-Beta zeolite after each run. Two peaks are observed in the derived thermogravimetric profiles (DTG) for all the used catalysts, as can be seen in Figure S10(b). The broad weak peak appears below 200 °C corresponding to the desorption of water adsorbed on catalyst, while the strong sharp peak at 420 °C is related to the burning of carbonaceous deposits. And calculated from TG profiles in Figure S10 (a), the content of carbon deposit reaches about 11 wt% for the fresh H-Beta zeolite. For each regenerated catalyst, the deposited carbon amount decreases very slightly after running. For instance, after regeneration for 6 times, the content of coke is about 10 wt% on the spent catalyst. So, after regeneration coke could be fully removed, and its impact on the catalytic performance could be negligible. These results further verify that the deactivation of catalyst should be caused by the dealumination of H-Beta zeolite other than the carbon deposit.

Conversion of other furans to aromatics

As shown in Figure 10, besides for the production of p-xylene, H-Beta-22 zeolite can also be used for the conversion of 2-methylfuran (MF)/furan and ethylene to toluene or benzene, respectively. But the catalytic performances for these two reactions are poorer than those for production of p-xylene. For the reaction of methylfuran and ethylene, the conversion of MF is 92 % with selectivity of 50 % to toluene after running 20 h. Similarly, the conversion of furan is 68 % with the selectivity of 28 % to benzene. The decrease in the conversion for methylfuran and furan may be due to the absence of methyl groups at the α -carbon positions of furan ring, lowering the reaction rate. The main byproduct

(see Figures S11-S12) is caused by the incomplete dehydration of the cycloadduct, alkylated product and the bipolymer of toluene or benzene. Further improvements in catalyst design require capability of complete dehydration of Diels–Alder cycloadducts to six-carbon aromatic rings and the abatement of polymers.

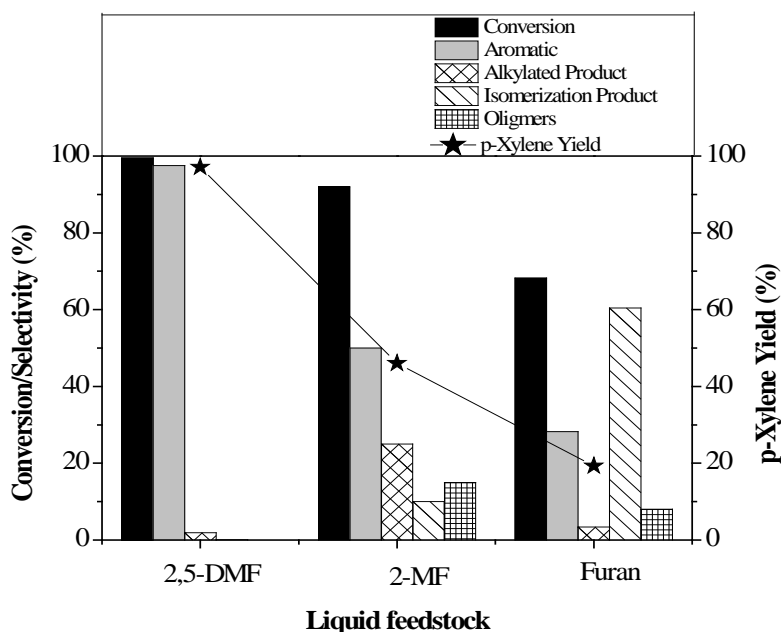


Figure 10 Catalytic performances for the production of p-xylene, toluene and benzene with different feed stocks over H-Beta-22 zeolite (catalyst weight=0.3 g, $C_{\text{feedstock}}=1.56$ M, $T=300$ °C, $t=20$ h)

Conclusions

The direct formation of p-xylene from 2,5-dimethylfuran and ethylene consists of a Diels-Alder cycloaddition followed by dehydration. Al-rich H-Beta zeolite and their dealuminated counterparts from organotemplate-free synthesis are highly active for this reaction. Especially H-Beta with Si/Al ratio of 22 is a superior catalyst with 2,5-DMF conversion of 99 % and p-xylene yield of 97 % under optimized reaction conditions. Its performances are even better than the commercial organotemplate-synthesized H-Beta zeolite with similar Si/Al ratio of 19. It also shows good stability and regeneration capability. After five successive regeneration cycles, the yield of p-xylene is still as high as 85 % without obvious dealumination from the zeolite lattice. NH_3 -TPD and ^{31}P MAS NMR spectroscopy with TMPO as the probe molecule show moderate Brönsted acid strength and Brönsted/Lewis acid ratio are benefit for the p-xylene production. Additionally, the formation of secondary pore system in dealuminated H-Beta zeolite detected

by ^{129}Xe MAS NMR facilitates the diffusion of product, which further improves reaction rate. This kind of H-Beta zeolite can also catalyze the reaction between methylfuran/furan and ethylene to produce toluene or benzene.

Experimental Section

Sample preparation

All the organotemplate-free Beta zeolites were provided by BASF SE, Germany, whose synthesis procedure was reported elsewhere.^[22,23] Briefly, organotemplate-free synthesis of Beta zeolites was carried out in aluminosilicate gel with molar ratio of $40\text{SiO}_2/1\text{Al}_2\text{O}_3/10\text{Na}_2\text{O}/570\text{H}_2\text{O}$ at a temperature of $140\text{ }^\circ\text{C}$ for 17-19 h in the presence of calcined Beta zeolite seeds with particle sizes of 60-100 nm. The resultant Al-rich Na-Beta zeolite was exchanged with 0.1 M NH_4NO_3 solution at $80\text{ }^\circ\text{C}$, then filtered, dried at $110\text{ }^\circ\text{C}$, calcined at $550\text{ }^\circ\text{C}$ to get Al-rich H-Beta (Si/Al=7). The dealuminated H-Beta zeolites with Si/Al= 22 and 36 were obtained by treating the parent Al-rich H-Beta with 4~15% HNO_3 aqueous solution at 50~100 $^\circ\text{C}$, then washed and filtered by deionized water, dried at $110\text{ }^\circ\text{C}$. Commercial zeolite Beta with Si/Al=19 from organotemplate synthesis (CP814C, NH_4^+ -form, Zeolyst) was converted to the H^+ -form by calcination at $550\text{ }^\circ\text{C}$ for 4 h. As demonstrated in our previous report,^[42] all samples have good BEA structure in XRD patterns, and their Si/Al ratios in the framework were determined by deconvolution of the corresponding ^{29}Si MAS NMR spectra. To repeated remove the extra-framework Al in H-Beta (Si/Al=22), 1.0 mol/L hydrochloric acid was added into the aqueous suspension of zeolites, then adjusted pH value to 1.0 in 3 hr. The suspension was stirred for 16 h at room temperature before filtration, then dried at $110\text{ }^\circ\text{C}$.

For the adsorption of trimethylphosphine oxide (TMPO, 99 %, Alfa), the samples were firstly subjected to a full dehydration under vacuum for 20 h. Subsequently, a known amount of TMPO dissolved in anhydrous CH_2Cl_2 was introduced into a vessel containing the dehydrated solid samples in a N_2 atmosphere, followed by removal of the CH_2Cl_2 solvent by evacuation at *ca.* $50\text{ }^\circ\text{C}$. To ensure a uniform adsorption of probe molecules in the zeolites, they were further subjected to thermal treatment at $165\text{ }^\circ\text{C}$ for 1 h. Finally, the samples were transferred into an NMR rotor and then sealed by a gas-tight endcap in the N_2 glove box. For the regeneration of H-Beta zeolites, the spent catalysts were heated in a tube furnace with 20 % O_2 at a flow rate of 30 ml/min at $550\text{ }^\circ\text{C}$ for 3 h.

Catalyst characterizations

Surface areas, pore volumes and pore size distributions were determined by the N₂ adsorption/desorption experiments at -196 °C on a Micromeritics ASAP-2020 analyzer. Before each measurement the samples were outgassed at 400 °C and below 10⁻³ Pa for 6 h.

NH₃ temperature-programmed desorption (NH₃-TPD) was carried out using a chemisorption analyzer (FINETECH, Finesorb 3010C, China) to detect the effluent gases using TCD. Before the measurements, the samples were pretreated in He stream at 500 °C and cooled down to the desired temperature. 5000 ppm NH₃ in He (100 ml/min) was introduced at 100 °C for 0.5 h, followed by He purging for 1.5 h, then the temperature was ramped from 100 to 700 °C at a rate of 10 °C/min.

All solid-state magic-angle-spinning (MAS) NMR experiments were carried out on an Agilent DD2-500 MHz spectrometer. Prior to performing ²⁷Al MAS NMR spectra all samples were hydrated completely in a desiccator with saturated NH₄NO₃ solution in order to reduce the “NMR-invisible” aluminum, then were packed into 4 mm ZrO₂ rotors and acquired at 130.2 MHz with a spinning rate of 14 kHz. The chemical shifts were referenced to 1 % Al(NO₃)₃ aqueous solution. The spectra were accumulated for 200 scans with $\pi/12$ flip angle of 0.34 μ s, and 2 s recycle delay. ³¹P MAS NMR single-pulse spectra were measured at 202.3 MHz with a speed of 14 kHz, $\pi/4$ excitation pulse of 1.2 μ s and recycle delay of 10 s. The chemical shifts were referenced to 85 % H₃PO₄. For the quantitative measurement of acidity, all samples were weighed, and the spectra were calibrated by measuring a known amount of (NH₄)₂HPO₄ performed in the same conditions except for the longer pulse delay of 90 s. ²⁹Si MAS NMR spectra were collected at 99.3 MHz using a 6 mm MAS probe with a speed of 4 kHz, 400 scans and recycle delay of 4 s. Chemical shifts were referenced to 4,4-dimethyl-4-silapentane sulfonate sodium (DSS). ¹²⁹Xe NMR spectra were obtained at room temperature operating at a frequency of 138.2 MHz. Typically, 400 acquisitions were accumulated for each spectrum with a recycle delay of 8 s and $\pi/4$ pulse of 2.1 μ s. Chemical shifts were referenced to xenon gas at zero pressure. Before xenon was adsorbed on the H-Beta samples, they were dehydrated at 400°C under vacuum, then a volume of xenon at known pressure was introduced into a 6 mm rotor. After adsorption equilibrium, the rotor was sealed, and ¹²⁹Xe NMR spectra were acquired under static condition or magic-angle spinning of 5 kHz. TG measurements were carried out on an America TA's SDT-Q600 Thermogravimetric Analyzer under air atmosphere with a flow rate of 20 ml min⁻¹. Samples were heated in the temperature range of 50–800 °C with a heating rate of 10 °C min⁻¹.

Catalytic reaction evaluations

The catalytic conversion of 2,5-DMF, 2-methylfuran or furan with ethylene was carried out in 50 ml stainless steel autoclave. Before reactions, the autoclave was purged by nitrogen, then the desired amount of H-Beta zeolites, 2,5-DMF 2-methylfuran or furan with solvent were transferred into the autoclave. The reactor was pressurized with ethylene gas, and the mixture was stirred at 1000 rpm with a mechanical stirrer to ensure facile mass transfer in the system, and heated up to the final temperature. After reactions, the liquid products and solid catalyst were separated by centrifugation. The products were analyzed using the gas chromatograph (Shimadzu, GC-2014C) equipped with a 30 m HP-5 capillary column and the flame ionization detector. The products were identified based on the retention times and response factors of the standard chemicals, and quantified using a known amount of n-decane as the external standard. The products were further identified by GC/MS (Agilent, HP6890/5973MSD) equipped with a 30 m HP-5 MS column.

Acknowledgements

We gratefully acknowledge the financial supports from the National Natural Science Foundation of China (Nos. 21673027, 21373035), the Fundamental Research Funds for the Central Universities in China (Nos. DUT16RC(3)002, DUT17TD04), the Program for Liaoning Innovative Research Team in University (No. LT2016001), and the International Network of Centers of Excellence (INCOE) project coordinated by BASF SE, Germany.

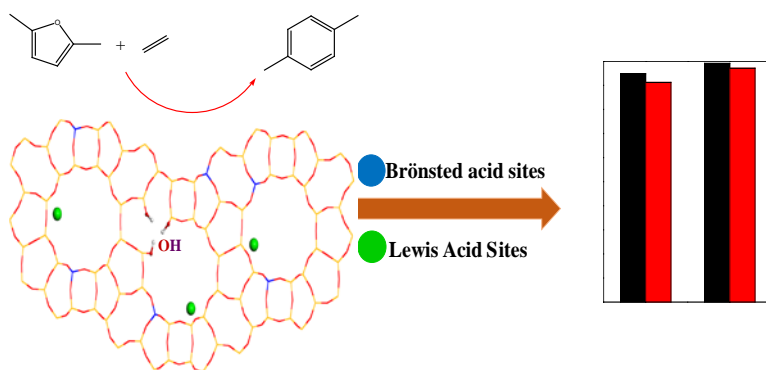
References

- [1] A. J. Ragauskas, C. K. Williams, B. H. Davison, G. Britovsek, J. Cairney, C. A. Eckert, J. R. Mielenz, *Science* **2006**, *311*, 484-489.
- [2] K. Sanderson, *Nature* **2006**, *444*, 673-676.
- [3] P. C. Bruijninx, B. M. Weckhuysen, *Angew. Chem.* **2013**, *125*, 12198-12206; *Angew. Chem. Int. Ed.* **2013**, *52*, 11980-11987
- [4] P. J. Dauenhauer, G. W. Huber, *Green Chem.* **2014**, *16*, 382-383.
- [5] P. T. Do, J. R. McAtee, D. A. Watson, R. F. Lobo, *ACS Catal.* **2013**, *3*, 41-46.
- [6] N. Nikbin, P. T. Do, S. Caratzoulas, R. F. Lobo, P. J. Dauenhauer, D. G. Vlachos, *J. Catal.* **2013**, *297*, 35-43.
- [7] N. Nikbin, S. Feng, S. Caratzoulas, D. G. Vlachos, *J. Phys. Chem. C* **2014**, *118*, 24415-24424.
- [8] C.-C. Chang, S. K. Green, C. L. Williams, P. J. Dauenhauer, W. Fan, *Green Chem.* **2014**, *16*, 585-588.

- [9] Y. P. Wijaya, D. J. Suh, J. Jae, *Catal. Commun.* **2015**, *70*, 12-16.
- [10] S. Dutta, M. Mascal, *ChemSusChem* **2014**, *7*, 3028-3030.
- [11] B. Saha, M. M. Abu-Omar, *ChemSusChem* **2015**, *8*, 1133-1142.
- [12] Y. Roman-Leshkov, C. J. Barrett, Z. Y. Liu, J. A. Dumesic, *Nature* **2007**, *447*, 982-985.
- [13] C. L. Williams, C.-C. Chang, P. Do, N. Nikbin, S. Caratzoulas, D. G. Vlachos, R. F. Lobo, W. Fan, P. J. Dauenhauer, *ACS Catal.* **2012**, *2*, 935-939.
- [14] D. Wang, C. M. Osmundsen, E. Taarning, J. A. Dumesic, *ChemCatChem* **2013**, *5*, 2044-2050.
- [15] C. C. Chang, H. Je Cho, J. Yu, R. J. Gorte, J. Gulbinski, P. Dauenhauer, W. Fan, *Green Chem.* **2016**, *18*, 1368-1376.
- [16] Y. P. Wijaya, I. Kristianto, H. Lee, J. Jae, *Fuel* **2016**, *182*, 588-596.
- [17] C. S. Triantafillidis, A. G. Vlessidis, L. Nalbandian, N. P. Evmiridis, *Microporous Mesoporous Mater.* **2001**, *47*, 369-388.
- [18] S. Yang, C. Yu, L. Yu, S. Miao, M. Zou, C. Jin, S. Huang, *Angew. Chem.* **2017**, *129*, 12727-12730; *Angew. Chem. Int. Ed.* **2017**, *56*, 12553-12556
- [19] J. Lynch, F. Raatz, P. Dufresne, *Zeolites* **1987**, *7*, 333-340.
- [20] A. Omegna, M. Haouas, G. Pirngruber, R. Prins In *Studies in Surface Science and Catalysis* (Eds.: R. Aiello, G. Giordano, F. Testa), Holand, Elsevier, **2002**, pp. 31-38.
- [21] V. Valtchev, G. Majano, S. Mintova, J. Perez-Ramirez, *Chem. Soc. Rev.* **2013**, *42*, 263-290.
- [22] B. Xie, J. Song, L. Ren, Y. Ji, J. Li, F. S. Xiao, *Chem. Mater.* **2008**, *20*, 4533-4535.
- [23] B. Yilmaz, U. Müller, M. Feyen, S. Maurer, H. Zhang, X. Meng, F. S. Xiao, X. Bao, W. Zhang, H. Imai, T. Yokoi, T. Tatsumi, H. Gies, T. De Baerdemaeker, D. De Vos, *Catal. Sci. Technol.* **2013**, *3*, 2580-2587.
- [24] G. Majano, L. Delmotte, V. Valtchev, S. Mintova, *Chem. Mater.* **2009**, *21*, 4184-4191.
- [25] B. Xie, H. Zhang, C. Yang, S. Liu, L. Ren, L. Zhang, X. Meng, B. Yilmaz, U. Muller, F. S. Xiao, *Chem. Commun.* **2011**, *47*, 3945-3947.
- [26] L. Xu, C. Shi, Z. Zhang, H. Gies, F. S. Xiao, D. De Vos, T. Yokoi, X. Bao, M. Feyen, S. Maurer, B. Yilmaz, U. Müller, W. Zhang, *Microporous Mesoporous Mater.* **2014**, *200*, 304-310.
- [27] Y. Zhu, B. Chen, R. Zhao, Q. Zhao, H. Gies, F. S. Xiao, D. De Vos, T. Yokoi, X. Bao, U. Kolb, M. Feyen, S. Maurer, A. Moini, U. Müller, C. Shi, W. Zhang, *Catal. Sci. Technol.* **2016**, *6*, 6581-6592.
- [28] T. De Baerdemaeker, B. Yilmaz, U. Müller, M. Feyen, F. S. Xiao, W. Zhang, T. Tatsumi, H. Gies, X. Bao, D. De Vos, *J. Catal.* **2013**, *308*, 73-81.
- [29] Y. Kubota, K. Itabashi, S. Inagaki, Y. Nishita, R. Komatsu, Y. Tsuboi, S. Shinoda, T. Okubo, *Chem. Mater.* **2014**, *26*, 1250-1259.
- [30] R. Otomo, U. Müller, M. Feyen, B. Yilmaz, X. Meng, F. S. Xiao, H. Gies, X. Bao, W. Zhang, D. De Vos, T. Yokoi, *Catal. Sci. Technol.* **2016**, *6*, 713-721.
- [31] R. Otomo, T. Yokoi, T. Tatsumi, *ChemCatChem* **2015**, *7*, 4180-4187.
- [32] Y. Wang, R. Otomo, T. Tatsumi, T. Yokoi, *Microporous Mesoporous Mater.* **2016**, *220*, 275-281.
- [33] G. L. Woolery, G. H. Kuehl, H. C. Timken, A. W. Chester, J. C. Vartuli, *Zeolites* **1997**, *19*, 288-296.
- [34] K. Leistner, K. Xie, A. Kumar, K. Kamasamudram, L. Olsson, *Catal. Lett.* **2017**, *147*, 1882-1890.
- [35] F. Gao, Y. Wang, N. M. Washton, M. Kollár, J. Szanyi, C. H. F. Peden, *ACS Catal.* **2015**, *5*, 6780-6791.
- [36] K. Leistner, A. Kumar, K. Kamasamudram, L. Olsson, *Catal. Today* **2018**, *307*, 55-64.
- [37] A. Zheng, S. J. Huang, S. B. Liu, F. Deng, *Phys. Chem. Chem. Phys.* **2011**, *13*, 14889-14901.

- [38] W. Zhang, S. Xu, X. Han, X. Bao, *Chem. Soc. Rev.* **2012**, *41*, 192-210.
- [39] A. M. Zheng, S. B. Liu, F. Deng, *Chem. Rev.* **2017**, *117*, 12475-12531.
- [40] H. M. Kao, C. Y. Yu, M. C. Yeh, *Microporous Mesoporous Mater.* **2002**, *53*, 1-12.
- [41] Q. Zhao, W. H. Chen, S. J. Huang, Y. C. Wu, H. K. Lee, S. B. Liu, *J. Phys. Chem. B* **2002**, *106*, 4462-4469.
- [42] R. Zhao, Z. Zhao, S. Li, W. Zhang, *J. Phys. Chem. Lett.* **2017**, *8*, 2323-2327.
- [43] J. L. Bonardet, J. Fraissard, A. Gedeon, M. A. Springuel-Huet, *Catal. Rev. Sci. Eng.* **1999**, *41*, 115-225.
- [44] W. Zhang, X. Han, X. Liu, H. Lei, X. Liu, X. Bao, *Microporous Mesoporous Mater.* **2002**, *53*, 145-152.
- [45] M. A. Springuel-Huet, J. L. Bonardet, J. Fraissard, *Appl. Magn. Reson.* **1995**, *8*, 427-456.
- [46] R. A. Ripmeester, *J. Magn. Reson.* **1984**, *56*, 247-253.
- [47] Y.-P. Li, M. Head-Gordon, A. T. Bell, *J. Phys. Chem. C* **2014**, *118*, 22090-22095.
- [48] Z. Zhao, S. Xu, M. Y. Hu, X. Bao, C. H. F. Peden, J. Hu, *J. Phys. Chem. C* **2015**, *119*, 1410-1417.
- [49] J. van Bokhoven, D. Koningsberger, P. Kunkeler, H. van Bekkum, A. Kentgens, *J. Am. Chem. Soc.* **2000**, *122*, 12842-12847.
- [50] X. Li, W. Zhang, X. Li, S. Liu, H. Huang, X. Han, X. Bao, *J. Phys. Chem. C* **2009**, *113*, 8228-8233.

Table of Contents



R. Zhao, Z. Zhao, S. Li, A.-N. Parvulescu, U. Müller, W. Zhang**
Excellent Performances of Dealuminated H-Beta Zeolites from Organotemplate-free Synthesis in Conversion of Biomass-derived 2,5-Dimethylfuran to Renewable p-Xylene

Direct synthesis of renewable p-xylene (PX) via cycloaddition of biomass-derived 2,5-dimethylfuran and ethylene was achieved on dealuminated H-Beta zeolite with PX yield of 97 %. Its excellent catalytic performances are closely related to the moderate Brønsted/Lewis acid ratio and unique pore structure.